IEEE Journal of Microwaves

Received 29 July 2021; accepted 19 August 2021. Date of publication 13 September 2021;
date of current version 7 October 2021.

Digital Object Identifier 10.1109/JMW.2021.3107423

Breakthroughs in Microwaves: Programmable Terahertz Chip-Scale Surfaces and Systems—An Interview With Dr. Kaushik Sengupta

ROBERT H. CAVERLY (Life Fellow, IEEE)

(Special Series Paper)

Electrical and Computer Engineering Department, Villanova University, Villanova, PA 19085 USA (e-mail: rcaverly@villanova.edu)

ABSTRACT This article is the next in the periodic Breakthroughs in Microwaves series. This series is intended to highlight recent accomplishments, especially to those new to the field, by researchers in microwave engineering that hold promise. Up until about 15 years ago, there was a distinct dearth of applications in the region between approximately 100 GHz and the infrared region except in radio astronomy. In the last 10 to 15 years, however, there has been significant research in this frequency range. Of particular interest are fully integrated solutions that utilize standard integrated circuit processes, made possible by the sub-millimeter wavelengths inherent to this frequency range. Increased parasitics and coupling make design using standard microwave techniques problematic when scaled to the THz range, but new thinking has emerged that looks at the full problem in an electromagnetic sense with full co-design of all elements needed. This article first provides the reader information on previous THz technology applications and then presents an overview of traditional antenna beamforming structures. This introduction is then followed by a discussion of new programmable chip-scale electromagnetic surfaces as one of the solutions for THz applications. This article ends with a lively discussion with one of the leaders in this technology, Dr. Kaushik Sengupta, who discusses further insight into this pioneering technique.

INDEX TERMS Beam steering, antenna radiation patterns imaging, sensor systems and applications, reconfigurable intelligent surfaces.

I. INTRODUCTION

A scan of a frequency allocation chart, such as from the US Dept of Commerce in [1], shows the frequency allocation spectrum ending at 300 GHz. Traditionally, the terahertz (THz) band is in defined with a start of between 100 and 300 GHz (3mm wavelength) through 10 THz (30-micron wavelength), at which point the infrared spectrum begins. This 300 GHz to 10 THz portion of the electromagnetic spectrum was therefore known as the 'THz gap' [2]. Up until approximately two decades ago, 100 GHz was about the highest frequency point research for most work outside of radio astronomy, whereas the infrared spectrum had been well-studied using lasers and similar sources in this frequency band. Early major application areas were in radio astronomy, where organic and inorganic complex molecules could be probed at frequencies up to 600 GHz at facilities such as the James Clerk Maxwell in Hawaii, USA or the Atacama Large Millimeter/ Submillimeter Array (ALMA) in the Atacama Desert in Chile [3]. However, about a decade ago, as sources were developed that could generate usable power levels, this so-called THz gap began closing rapidly. Besides the opportunities for communications systems in this frequency range, the THz band is intriguing because over the 0.1 to 10 THz range, there are significant physical effects that can be uniquely probed using electromagnetic waves. Since the THz band is just below the infrared and optical frequency bands, THZ signals can be thought of in terms of both waves and particles (or 'wavicles' as my university physics professor once said) as

This work is licensed under a Creative Commons Attribution 4.0 License. For more information, see https://creativecommons.org/licenses/by/4.0/

opposed to purely electromagnetic waves at lower frequencies. These THz particles, or photons, still exhibit very little energy compared with higher frequency optical and X-rays as described by the simple Planck-Einstein energy relation $E = hf$ where h is Planck's constant and f is the frequency in Hz. Because of this dual nature, radiating structures in the THz band can be based on electromagnetically described active antenna structures similar to those seen at lower frequencies (see, for example, 4-7]), or optically described lens-type structures (usually dielectric layers or conducting meshes/gratings [8]–[11]) that manipulate a wave front in a desirable fashion. Because of the small wavelengths, the structures associated with THz electronics, antennas and systems will also be physically small, making them potentially ideal for fully integrated products since a 1 THz electromagnetic wave has a free space wavelength of 0.3 mm (less in a dielectric). This allows more than three full wavelengths of structures to be placed on a single semiconductor die 1mm by 1 mm. THz applications can be found in wide-ranging fields such wireless communication, spectroscopy, sensing and imaging [11]–[17]. THz signals are ideal for material spectroscopy due to their low photon energy and ability to propagate through samples without causing the damage that an ionizing wave could, which also coincides with the energy level differences, allowing unique methods of probing various material properties that cannot be probed by lower frequency spectroscopic methods [18]–[20]. The emergence of integrated circuit power sources in the 0.1 to 1.0 THz range [21]–[35] are replacing high power millimeter-wave circuits feeding multiple frequency multipliers [36]–[42]

The ability to direct electromagnetic energy in a desired direction, or receive a signal from a preferred direction, is a fundamental area of THz research since it finds utility in many of these applications. Traditional applications based on antenna-like structures span the frequency spectrum, with antenna pattern changes for 1 MHz AM broadcast stations to electrically steered beams in the microwave and millimeter range. In these cases, strategically placed discrete antenna elements (vertical monopoles or patches, for example) are arrayed in such a manner that if fed by signals with certain amplitudes and phases, the main lobe can be scanned over a wide angle. While this approach is useful into the mm-wave band, as research continues to push the THz frontier, the physical spacing of the elements and the parasitics associated with the individual elements as well as coupling between elements start to make these types of structures more problematic to design. From an electromagnetic perspective, there are other differences compared with lower frequency operation. For example, a diffracting THz signal may have different propagation characteristics than its modulation sidebands, implying that a MIMO antenna array may collect different information bands even if all propagation is considered line of sight [43]. These differences help explain the interest in, and challenges of, current and future THz research.

Recently, there has been significant work done in novel approaches to beamforming in the THz range. Rather than individual antenna elements, a reconfigurable and programmable

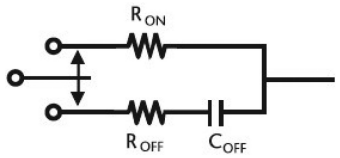

FIGURE 1. Simplified switch model showing the low and high impedance switch states with actuator.

electromagnetic surface has been employed that provides control of surface currents to dynamically alter the radiation pattern of the antenna [12]. To assist the reader in understanding some of the issues involved in THz beamforming, this paper will review some of the key sub-THz technologies for conventional beamforming electronics. The sub-THz technologies covered will be elements used for reconfiguration (primarily switches) and fundamental antenna beamforming concepts. These fundamental concepts will then be applied to help in the understanding of the operation of programmable and reconfigurable THz surfaces for transmit and receive. To conclude the article, a discussion of the pioneering work in programmable and integrated THz electronics will be presented along with an interview with a well-known researcher in this field, Dr. Kaushik Sengupta of Princeton University, USA.

II. RECONFIGURABILITY

Steering a beam electronically involves interplay between the separation of the individual antenna elements and how the individual elements are fed (in both amplitude and phase). Mechanical relays and even manually thrown switches were used in the earliest antennas but more modern means using solid-state components such as field effect transistor (FET)-based switches PIN diodes, microelectrical mechanical systems (MEMS), and switches based on phase-change materials are widely employed [44]–[53]. Among the main considerations for these types of reconfiguration elements are the loss each one introduces into the system, the speed in which they switch, the energy required to switch, the energy required to maintain the system in the switched state, power handling and, especially for high frequency use, the parasitics of the elements. A figure of merit for semiconductor switches, the broadband switch cutoff frequency F_C is computed based on the low value of on-state resistance R_{ON} and the low value of off-state capacitance C_{OFF}: [54]

$$F_C = \frac{1}{2\pi R_{ON} C_{OFF}},\ F_C = \frac{1}{2\pi\sqrt{R_{ON} R_{OFF}} C_{OFF}}, \quad (1)$$

the form of (1) depending on the knowledge of primarily R_{OFF} (see Fig. 1).

Depending on switch type, the origins of the resistances and capacitance are different. For PIN diodes, R_{ON} originates from the conductivity modulation in the intrinsic (I) region with the applied DC forward current, leading to the standard expression for the PIN diode high frequency resistance [54]:

$$R_{ON} = \frac{W^2}{2\mu_a I_{DC} \tau};\ C_{OFF} = \frac{\varepsilon A}{W}. \quad (2)$$

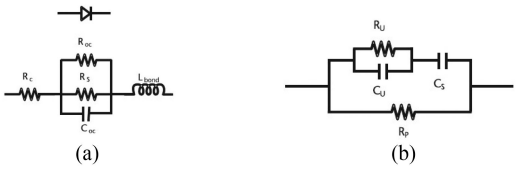

FIGURE 2. (a) Simple forward bias PIN diode RF equivalent circuit; (b) simple reverse bias PIN diode RF equivalent circuit.

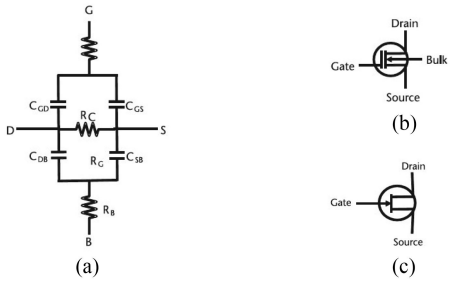

FIGURE 3. (a) RF equivalent circuit for FET control element; (b) MOSFET; and (c) MESFET schematics.

The off-state capacitance C_{OFF} is governed by the width of the I-region when the I-region is fully depleted during reverse bias. The additional resistance R_{OFF} takes into consideration other resistive losses in the device. More detailed equivalent circuits for PIN diodes in both switch states are shown in Fig. 2.

For FETs, these equivalent circuit elements vary in origin depending on the type of FET: MOSFET, MESFET or HEMT. However, in general, the conduction properties of the channel between the drain and source can be modulated with an applied gate voltage, with the resulting R_{ON} being governed by the physical geometry of the device. Similarly, the physical geometry governs the various capacitances between the different terminals of the devices, leading to an effective C_{OFF}, being a complex blend of the various capacitance values. MOSFETs exhibit particularly high values of drain and source capacitance due to the nature of the diffused regions that make up those nodes; these capacitances can be reduced by using SOI (silicon on insulator) processes as opposed to bulk silicon technology nodes. Fig. 3 shows a simplified equivalent circuit for these devices. In switching applications, all FETs operate with low drain-source voltage V_{DS} and therefore operate in the so-called linear or triode region. Using simple I-V expressions for these devices shows that the linear on-state resistance, denoted by R_C in Fig. 3, is similar to the transconductance of the same device when operating in its amplifying state; that is, $R_C = 1/g_m$. This is an especially important observation because FETs are often described by their unity gain frequency f_{max}, which includes the transconductance parameter g_m [54]:

$$f_{\max} = \frac{g_m}{2\pi C_{gs}};\ R_C = \frac{1}{2\pi f_{\max} C_{gs}} \tag{3}$$

and therefore improving f_{max} through technology improvements also improves the on-state R_C. The various capacitances

TABLE 1. Summary of Reconfigurable Element Characteristics

	PIN Diode	FET	MEMS
Switching speed	High	High	Medium
Integration	Low to Medium	High	Medium to High
Power Handling	High	Medium	Medium
Switching energy	High	Low	Low
Switching Type	Current	Voltage	Voltage
FC	Medium	High	High

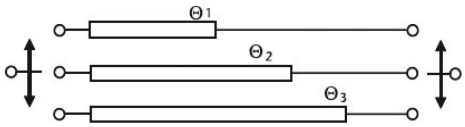

FIGURE 4. (a) Simple forward bias PIN diode RF equivalent circuit; (b) simple reverse bias PIN diode RF equivalent circuit.

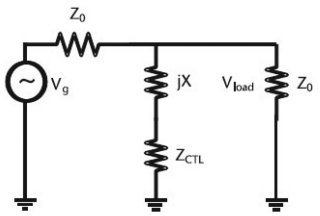

FIGURE 5. Circuit diagram for single element switched phase shifter.

vary in magnitude with the FET technology, MOSFET or MESFET. MOSFET parasitic capacitances are higher than their MESFET counterparts, with SOI-MOSFET capacitances lower than bulk-MOSFET technology nodes.

After several decades of intense research, MEMS have achieved F_C values well into the tens of THz [55], [56] with applications such as waveguide bandpass filters and phase shifters [57] at frequencies of approximately 300 GHz and 500 GHz, respectively. In addition, many of the early limitations of MEMS such as low switching cycles and packaging issues are currently improving, with commercial RF MEMS exhibiting switching cycles in excess of one billion and power handling in the tens of watts [55], [56]. Each of these reconfiguration schemes has their advantages and disadvantages; Table I shows a summary of some of these characteristics for the general switch types.

These switching elements are frequently used in phase shifters in RF beamforming applications. Phase shifters can be switched transmission line sections (Fig. 4) or switched circuit elements (Fig. 5). In the switched line section phase shifter, the elements switch in transmission lines of different electrical length to modify the phase angle as shown in (4). Insertion loss is governed by the length of the line, which is usually low, but adjustments to length are often required since the off-state switch elements influence the effective electrical

length introduced by the transmission line elements.

$$\Delta\Theta_i = 2\pi\frac{L_i}{\lambda_g} = 360^\circ\frac{L_i}{\lambda_g} \tag{4}$$

A simpler, and more compact, phase shifter is the single reactive element phase shifter (Fig. 5) where X is the reactance of the shunting element and controls the degree of phase shift. For larger phase shifts, X should be smaller than Z_0 but at the same time, large enough so that the control element impedance Z_{CTL} does not overly influence the overall shunting reactance. This small X value unfortunately reduces the transmission coefficient T through a reflective mismatch, therefore limiting the maximum phase shift to approximately 45°, as shown in (5) [40]. A modification of this basic phase shifter uses two shunting elements separated by a quarter wavelength transmission line. This quarter wavelength transmission line provides cancellation of the reflections from the two shunting elements at the input, thereby improving the match and the transmission through the phase shifter [57].

Active phase shifters have been developed that extend into the THz bands. Vector modulators [58], [59] are often employed as they show a good blend of gain, linearity and area performance characteristics and employ switching transistors and controlled current sources to provide a wide range of phase shifts. Good quality couplers and baluns at the input and output of the circuit are necessary for good amplitude and phase balance as well as insertion loss and bandwidth considerations [57].

$$T = \sqrt{\frac{4X^2}{Z_0^2 + 4X^2}}e^{-j\tan^{-1}\left(\frac{Z_0}{2X}\right)} \tag{5a}$$

$$\Delta\Theta = \tan^{-1}\left(\frac{Z_0}{2X}\right) \tag{5b}$$

III. ANTENNA ELEMENTS

The earliest investigations of directive communication long wave antennas go back to Marconi's original experiments. An excellent summary of these early directive communication antennas can be found in a paper by Beverage, Rice and Kellog [60]. Practical applications of mechanically oriented antennas go back nearly 100 years to the work by Yagi and Uda [61] from Tohoku University, Sendai Japan, who looked at the impact of parasitic elements (reflectors and directors) to provide directionality, with their original array and pattern shown in Fig. 6.

Volume 12 of the famous 28-volume MIT Radiation Laboratory (RadLab) series was devoted to the mathematics of directive antennas and the mathematics governing linear arrays of antennas [62]. In the general scenario covered in this reference, a linear array of geometrically spaced antennas is fed with signals of differing amplitudes and phases. Proper selection of the feed amplitude and phase as well as the physical separation leads to a beam that can be electronically steered. In these arrays for beamforming at the final

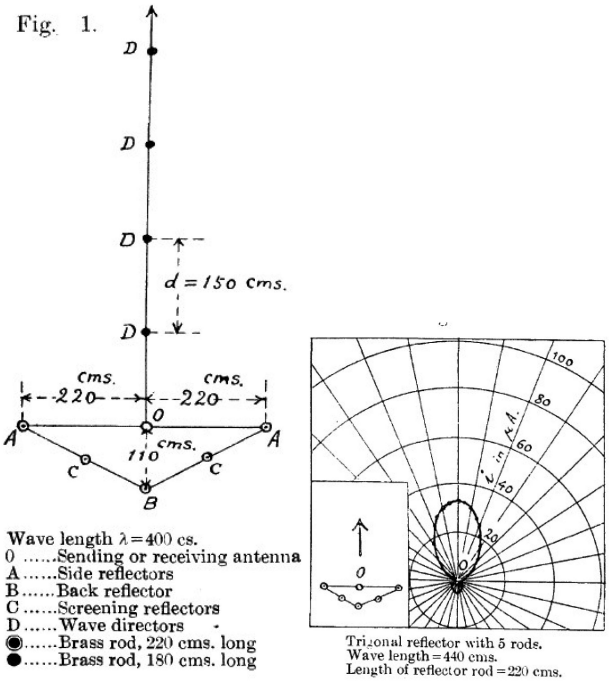

FIGURE 6. Proposed antenna and radiation pattern from the original Yagi-Uda paper [61].

RF frequency, the phase of the feed signal is often adjusted using reconfigurable phase shifters such as described in the previous section. More recently, beamforming has taken two tracks: analog and digital beamforming [65]–[68]. However, the concept is essentially the same: adjust the amplitude and phase of the antenna element feed points to steer the beam in a preferred direction, whether it is done through digital signal processing algorithms or at RF frequencies. Since these beginnings, the engineering and science of antenna directivity and beamforming has expanded exponentially so that now a search on IEEE Xplore alone provides more than 280,000 entries spanning various antenna types over the kHz to THz range. Two-dimensional arrays of antennas are also employed.

Arrays of these individual elements interact through phasing in both feed and physical separation and provide the ability to steer the main lobe of the antenna in desired directions. Fig. 7 shows N radiating elements in a linear array, each being fed with E_i amplitude and Φ_i phase, to be received at point P in the far field. The term in (6) is called the array factor, which, when combined with the field pattern of the individual elements in the array $E_{ANT}(\Theta, \Psi)$ provides the pattern and directivity of the entire array.

$$E_{TOT} = \sum_{n=0}^{N-1} E_n e^{j\varphi_n} e^{j\frac{2\pi d(N-1-n)}{\lambda}\cos\Theta}$$

$$= E_{ANT}(\Theta, \Psi)\sum_{n=0}^{N-1} E_n e^{j\varphi_n} e^{j\frac{2\pi d(N-1-n)}{\lambda}\cos\Theta} \tag{6}$$

Fig. 8, for example, shows an ideal microstrip patch antenna electric field pattern along with the array factor and combined

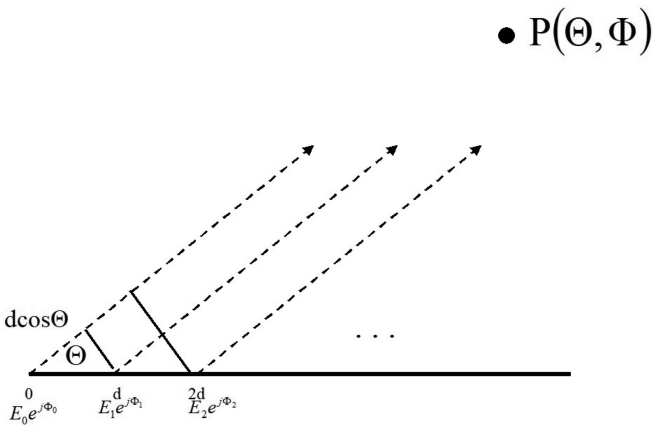

FIGURE 7. Geometry for the linear antenna array.

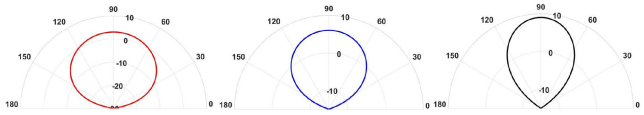

FIGURE 8. (a) Patch antenna pattern; (b) array factor; and (c) overall pattern of ideal microstrip patch antenna array. Degrees and dB are indicated.

far-field electric field pattern for a two-element array using (6).

Over the years, antenna types ranged from wire or metal tubing antennas, through conformal antennas to dielectric lenses for THz and near-THz applications. Early conformal antennas [69] on dielectric substrates included dipole antennas [70], slot antennas [71] and the now-widely used and studied microstrip patch antenna [72] (see Fig. 9) (more than 39,000 entries in IEEE Xplore [73]), which also included a short discussion of obtaining a circular polarization. Indeed, the author in [72] ended the article with the statement "Antennas of this type should be very useful in phased arrays".

In all cases, however, it is the distribution of current on the antenna element that governs the radiation pattern and radiation efficiency [74]. This can be seen at the most fundamental level by the dependence of the magnetic vector potential $\vec{A}$ for the infinitesimal antenna [74]:

$$\left|\vec{A}\right| = \frac{\mu I(z)}{4\pi r} dz \tag{7}$$

from which the electromagnetic fields can be derived. The current distribution on the antenna *I(z)* can be a constant value for very small monopoles, through a sinusoidal function for dipoles to complex patterns in microstrip and other antennas. For microstrip antennas, much work is devoted to understanding these surface currents through simulation to design the radiation pattern from the antenna (see Fig. 10 for example).

As frequencies moved from millimeter waves into the THz realm, the combination of increased coupling between the antennas, increased losses and phase shifts in the interconnects between antennas, and the increased need for integrating the antennas with the electronics on a single semiconductor die

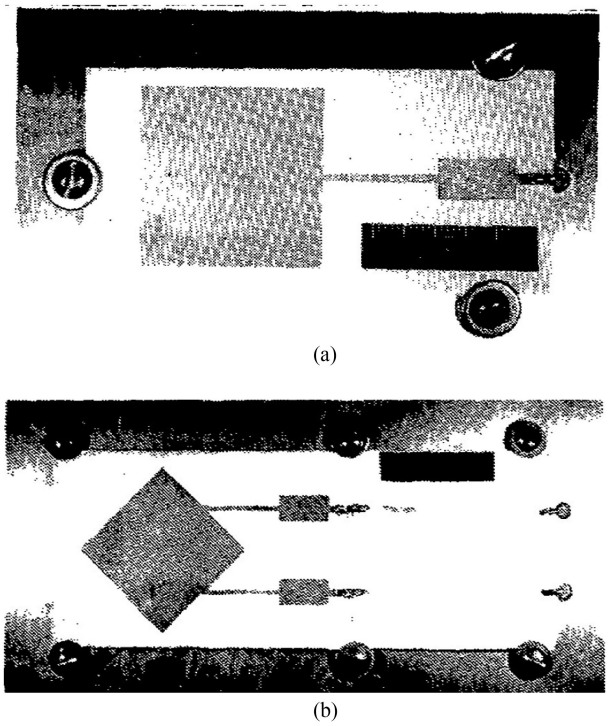

FIGURE 9. Originally reported microstrip antenna: (a) L-band antenna; and (b) circularly polarized version of the antenna [72].

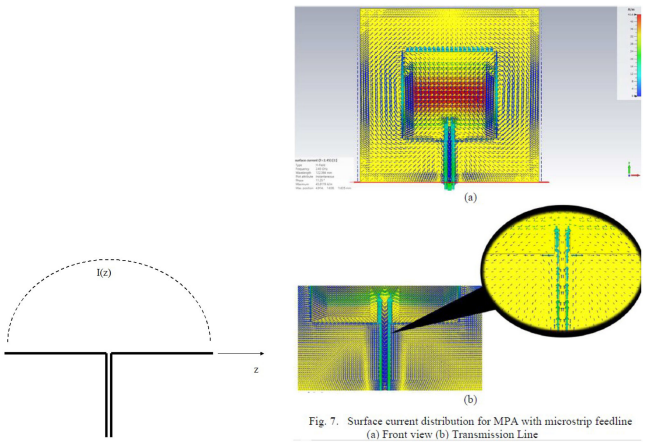

FIGURE 10. (a) Current distribution on simple dipole antenna; and (b) surface current on a microstrip patch antenna [76].

required re-imagining the concept of a phased array antenna designed based on longer wavelength signals. As frequencies increase, especially into the THz band, substrate and other coupling effects dramatically increases, causing significant departures in operation from these straightforward explanations. An excellent overview of THz antenna technologies can be found in [75].

IV. PROGRAMMABLE ELECTROMAGENTIC SURFACES

A novel approach in solving this problem has been advanced by Dr. Kaushik Sengupta of Princeton University, Princeton,

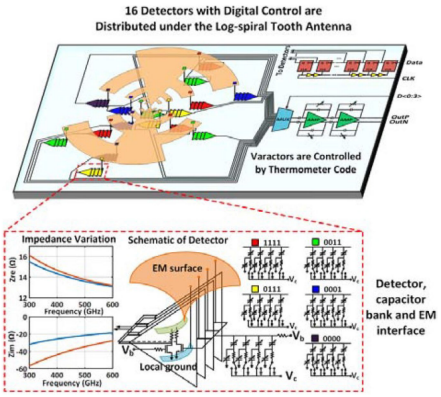

FIGURE 11. **Programmable electromagnetic surface [79].**

NJ USA using programmable smart electromagnetic surfaces that can be reconfigured for a particular application or beam type. Rather than using reconfiguring elements (in this particular application, MOSFETs) to switch in various phase shifting elements, this unique approach for THz sensing uses an array of MOSFET detectors and five-state capacitor switching banks, depending on the application, to change the conditions on the surface at various locations, thereby changing the surface current distribution in both amplitude and phase, and hence its sensor reception properties (Fig. 11). In [77], the programmable sensor exhibits 16 different switching elements distributed along the electromagnetic surface that gives rise to 5^{16} different permutations to control the surface current distribution. A blend of gradient decent and random search optimization methods is used to determine the optimum states of the reconfigurable elements for a specific receive pattern, although this may not be a global optimum as stated by the author. The signals from the 16 detectors are then processed on the same chip as the surface and switching electronics, all on a chip 2 mm by 1 mm in a standard 65 nm CMOS process. The chip consumes a total of 10 mW of power [77]. Another type of programmable electromagnetic surface is outlined in [78], using 84 circuit points distributed along the electromagnetic surface to program the surface currents to yield the desired formed beam.

V. A CONVERSATION WITH DR. KAUSHIK SENGUPTA

Dr. Sengupta agreed to be interviewed for this Breakthroughs in Microwaves' article in July 2021 via teleconference. The author appreciates Dr. Sengupta's time and willingness to share with the readers some of his work and insights into these new techniques. Looking through Dr. Sengupta's extensive publication record shows a significant level of achievement of developing sensors for a variety of applications in the THz frequency range [12], [77]–[85]. The questions posed to Dr. Sengupta focused on this effort. This section will present the interview in a familiar question and answer format. The interview responses were edited for length.

Robert Caverly [RC] –Thank you for taking the time to allow me to ask you some questions about your research work. In reviewing your publications, you started out looking at standard arrays of individual antenna elements, moving towards these programmable electromagnetic surface structures. What eventually led you to this approach?

Kaushik Sengupta [KS] – About ten years ago when I started my graduate studies, we started to think about how we generate power at frequencies at hundreds of GHz. This was before the start of 5G, and 6G was not even on the horizon yet. Generating power at these frequencies meant that we needed to think about ways to generate power beyond f_{max}. We were also thinking about how not only generating power but also how to do we get the power into and out of the chip. I decided to think outside of the traditional types of circuits and systems, because these conventional discrete circuits and system blocks are sub-optimal in their own ways.

The first approach was to forget about the kind of antennas we know and think about a way to synthesize the optimal surface currents in a silicon chip to get the required THz beamforming, and then think about ways to synthesize those currents through a combination of circuits, antennas, and other active elements. This brought about the thinking of so-called electromagnetic and circuit co-design rather than thinking about linking individual discrete sub-systems as is currently done at frequencies below the THz band. This resulted in one of the earliest beamforming arrays on-chip close to 300 GHz. Of course, researchers have gone on from there and have worked to get more power from silicon devices, which is something that we also work on. There is a lot of advancement in this area.

This then led to us to think about the whole communication system, including the channel. It is important to not think of just a transmitter and receiver (or multiples of each) and a static channel, which is subject to blockages, but it is interesting to think of ways one can program the channel itself. Imagine multiple transmitters and receivers in a system, and then some sort of blocking occurs. What we can now think of is that the transmitter can direct its signal to a smart reflector somewhere, and that reflector can act as a beamformer to direct the power to the receiver, thereby closing the link and mitigating the blocker. We don't have to then rely on fixed reflectors but can now rely on a smart surface to close the link. These smart reflectors or programmable surfaces can be quite sophisticated—they can create single or multiple beams, allow full duplex operation, and they hardly dissipate power since they use passive reconfigurable elements. These reflector arrays have been researched to the hilt in the microwave community but are exceedingly challenging to realize above 100 GHz. We showed a way to create them at 300 GHz with tiled silicon chips. These surfaces are passive themselves, and only the digital control consumes the power. One can imagine a distributed network with multiple transmitters, receivers and surfaces that are resilient to blockages, or other issue that reduces link performance.

[RC] – You have done a lot of work on programmable reconfigurable surfaces, but I want to make sure I understand the differences between the two major works that you have done on programmable sensors and metasurfaces.

[KS] – In the programmable sensor, we wanted to have a THz chip-scale sensor that can adapt to the incident field properties and then detect the incident power. The sensor is designed using a distributed programmable surface.

Things are a little different for the metasurface, where in this case, the incident field comes in and a different field goes out and so no power is absorbed by the surface. All the structure does is impart changes to the amplitude and phase conditions on the surface boundary at sub-wavelength scales, by changing the scattering conditions of the surface electronically.

So in both cases we are using a distributed programmable surface, but one is detecting power, the sensor, while the other is changing the electromagnetic field configuration to create the beamforming, the metasurface.

In a traditional sensor, we start with a resonant antenna that has a certain impedance and then we match that to the input stage of the receiver and then go down the chain. Here, the idea is the following, how do you make the surface programmable to the incident field properties? Well, one needs to electronical modify and control the surface currents to the incident field properties. So, imagine an electromagnetic surface acting as an antenna, with tiny detectors distributed over the surface where each has an ability to make some small impedance changes. Now, you have a system, where collective small changes can lead to large changes in the system properties. One big question then arises: what is the optimal antenna structure for such programmable surfaces? A microstrip patch or log periodic structure? It turns out no one knows! Interesting questions then come up on the optimal structures, the optimal number of detectors, the optimal placement of the detectors and how much variability do you have or can be handled. Theoretical understanding of the fundamental questions is the interesting problem because with the THz antenna on the chip, it is a new ballgame.

[RC] – Given all the degrees of freedom in the switching arrangement for surface currents, I see you used a combination of gradient descent and random search algorithms. What were some of the variables in the cost function for the search algorithm?

[KS] – An interesting, fundamental question. I like the quote, "there are no solutions, only trade-offs". But some trade-offs are better than others, depending on what you want to. So, once you get rid of the idea of the antenna being static and focus then on a reconfigurable electromagnetic surface or interface, it is not clear what the design methodology and trade-off space looks like. The search space is highly non-convex and so we have to rely on heuristic algorithms that gives us reasonable coverage of the search space, and not get trapped in a local minimum. In the work on programmable THz sensors, we wanted to make the sensor operate over the range from 0.1 to 1 THz, and exhibit a +/−45 degree angle of incidence and polarization. Therefore, the cost function would be a blend of all of these features simultaneously. In our approach, we first captured the detailed S-parameters of the passive electromagnetic structure as a massive multiport network with 84 different ports spread out over the surface by simulating over the frequency range using HFSS. We then varied the impedances through switched capacitor banks seen at each port to generate the desired surface currents to obtain the performance that we sought. We only needed the one detailed multiport electromagnetic simulation of the passive surface, and then we could use much faster algorithms from the signal processing community for the search. No one really knows the optimal set of parameters, but we did get a solution that provided useful performance over all of the parameters of the search.

[RC] – Can you tell me a little about the susceptibility of the electromagnetic surface to heating effects, say deformation of the surface, with the electronics on the substrate?

[KS] – Great question. We have to have packaging that is thermal aware and packaging is one of the big issues of high frequency systems. Since the dimensions of the chip are of the order of a wavelength in this frequency regime, you are now packing electronics in a small space, and so heat dissipation is an important consideration. Several researchers have looked into this. In our work, for example on the programmable surfaces, the situation eases out a bit since they are very low power and use switches and other passive elements that program the electromagnetic surface to reflect beams to connect links. They are also great for imaging applications because the surface can create complex beam patterns, instead of just blindly scanning, and from the scattering fields, you get your imaging done much more quickly. Applications are many-fold, not just for communications but also imaging and sensing. For transmit arrays, however, power dissipation is always a factor and must be considered.

[RC] – Another question that I had while reading your work is how fast the surface can be reconfigured. You use MOSFET switches in your reconfiguration structure and so those of course have a finite switching speed.

[KS] – There are actually two parts to answering this question. The MOSFET switches themselves switch very quickly, on the order of nanoseconds, and so the surface can be reconfigured very quickly. The other issue, however, is the time it takes to decide on the type of surface currents that need to be created on the programmable surface. This decision time between identifying the received incident field pattern on the programmable surface and the response time to create the new field can be much longer than the actual switching time and of course then depends on the processing speed of the decision algorithm.

[RC] – Speaking of CMOS, in some of your work you used 65 nm CMOS. Can you mention why smaller geometry CMOS may not be helpful at higher frequencies?

[KS] – Smaller geometries below 65nm can be helpful at higher frequencies, 45 nm or 28 nm depending on the applications. We like to concentrate on architectures and methodologies that are technology node agnostic in some sense. Below about 65 nm silicon CMOS, you really do not get the corresponding dramatic increase in f_{max} with gate length, as was true for longer channel lengths. At this point, the gate and contact resistances are now major issues inhibiting the increase of f_{max}. You will get some advantage of going to 45 or maybe 28 or 22 nm, but it is not dramatic. The SiGe front, however, does look more attractive for multiple reasons. In the range of works we demonstrated in the 65-nm process, they will probably work better at 45nm or 28 nm, but it will still be an adequate performer at 65 nm.

[RC] – For creating these programmable structures in silicon, was any post-processing required or was this a typical 65nm CMOS node?

[KS] – Interfacing these high frequency chips to the external world is very important. For the programmable THz sensor work, for example, we wanted to create sensors that can adapt themselves based on all the properties of an incident THz-field, include its spectrum, angle of incidence, and polarization. Therefore the THz interface that is exposed to the world, and receives the incident field is very important. For the THz metasurface which can reflect, transmit or otherwise change its scattering characteristics electronically, packaging is critical—the whole electromagnetic environment has to be considered, what type of package the chip goes in, what goes in front and what goes in back of the die. Lenses, quartz plates, back plates, all have to be taken into account in the electromagnetic co-design with the circuitry and structures.

[RC] – In your programmable electromagnetic surface, can you tell us a little bit about the design decisions involved in choosing the concept of capacitor banks.

[KS] – The use of switch capacitor banks is actually fairly common in the integrated circuit world, because capacitors are relatively high-quality factor reactance elements, and it is relatively easy to do a thermometer-code for digital control of the capacitors. The challenge is not so much the stand-alone design of the detector and the capacitor bank. The detector is attached to the electromagnetic surface as is the capacitor bank for boundary condition adjustment and they now both must be part of the co-design and not done separately because of the complex electromagnetic interactions of these circuits on the final surface current pattern. Here, you do not have the standard case where you have a single port antenna that you conjugate match to the receiver. Once it becomes multiport, for example for the 16-port THz sensor surface, you have 16x16 antenna matrix, a 16x16 receiver matrix, and so the question becomes what impedance do you match to? There are methods to this 'madness', and the location of the circuits, the sizing of the elements in the detector and switches, the sizing of the capacitors, all have to be taken into account for the overall system to be matched. Remember, the angle, polarization and frequency range of the incident field's search space is huge, and so these component characteristics must be co-designed to address performance and the related element sizes, locations and other factors.

[RC] – I appreciate the time from your busy schedule to address some of these questions to provide the reader better insight into the programmable surfaces and their use in THz applications. Do you have any last thoughts that you would like to share with the readers?

[KS] – Yes, thank you very much for the opportunity. Let me say a little bit about what some of the opportunities may be for the rich world of wireless sensors, surfaces and the like. As we know, the application space for millimeter waves is increasing rapidly specially in the sensing domain, and also in the communication front 5G, satellite communication and others. So it is only a matter of time before a large number of similar, and new, applications move to sub-millimeter and THz bands. At these higher frequencies, we really do need to adjust our thinking about new design methodologies given transistors are not great at these frequencies. If you think about some of the applications such as automotive radars, or intelligent sensors in self-driving cars, drones, warehouses, robots, cyber physical systems, these are not well-controlled environments and so the systems will need to adapt to the changing conditions. For example, you may need to collect information over a range of frequencies to be better able to understand the environment, and so now you are looking at a multi-spectrum or hyper-spectral environment. We do some version of this already with millimeter-wave radars, Lidars (light detection and ranging), and cameras for self-driving cars. But you need a broader cast across the spectrum for the wide diversity of new applications. Therefore, the concept of traditional stand-alone transceivers at fixed frequencies has limitations on what they can actually sense in a complex environment.

[RC] – This sounds like a sensor fusion problem.

[KS] – Yes, that is part of it, but the data actually need to be relevant to fuse, and so the sensors need to perform over a broad swathe. This could be spectrum, spatial field distribution, polarization or what have you. The question now becomes, how do you build these interfaces or surfaces that operate in an intelligent way, by which I mean they have the ability to collect information, understand it, and then make a decision. This makes for a rich playground for new system design research. I like to call this 'electromagnetic fields to information' or vice versa, and these could be at radio frequencies, microwaves or the THz band, depending on the problem. How you connect these two, fields to information, is how I like to think about these new applications.

ACKNOWLEDGMENT

The author would like to thank Dr. Kaushik Sengupta for his time in agreeing to the interview and providing further insight into programmable electromagnetic surfaces, sensors, and systems for THz applications.

INTERVIEWEE BIOGRAPHY

KAUSHIK SENGUPTA (Senior Member, IEEE) received the B.Tech. and M.Tech. degrees in electronics and electrical communication engineering from IIT Kharagpur, Kharagpur, India, in 2007, and the M.S. and Ph.D. degrees in electrical engineering from the California Institute of Technology (Caltech), Pasadena, CA, USA, in 2008 and 2012, respectively. He joined as a Faculty Member with the Department of Electrical Engineering, Princeton University, Princeton, NJ, USA, in 2013, where he is currently an Associate Professor and Director of Graduate Studies. His current research interests include high-frequency ICs, electromagnetics, and optics for various applications in sensing, imaging, and high-speed communication. Dr. Sengupta received the DARPA Young Faculty Award in 2018, the Bell Labs Prize in 2017, the Young Investigator Program Award from the Office of Naval Research in 2017, the E. Lawrence Keys, Jr./Emerson Electric Co. Junior Faculty**.** Award from the Princeton School of Engineering and Applied Science in 2018, and the "Excellence in Teaching Award" in 2018 nominated by the Undergraduate and Graduate Student Council in the Princeton School of Engineering and Applied Science. He was a recipient of the Charles Wilts Prize in 2013 from the Department of Electrical Engineering, Caltech, for the best Ph.D. thesis, the Prime Minister Gold Medal Award of IIT in 2007 and a recipient of the inaugural Young Alumni Achievement Award from IIT Kharagpur in 2018. He is the Chair of the Emerging Technologies Sub-Committee in the IEEE Custom Integrated Circuits Conference (CICC), served on the steering committee in IEEE International Microwave Symposium in 2021, and previously served in similar roles in the IEEE European Solid-state Circuits Conference (ESSCIRC) and Progress in Electromagnetics Research (PIERS). He was a co-recipient of the IEEE RFIC Symposium Best Student Paper Award in 2012 and the 2015 Microwave Prize from the IEEE Microwave Theory and Techniques Society. He is a member of the MTT-4 Committee on Terahertz technology, a Distinguished Lecturer of the IEEE Solid-State Circuits Society from 2019 to 2020, and a Distinguished Lecturer of the IEEE Microwave Theory and Techniques Society from 2021 to 2023. He is a recipient of the Outstanding Young Engineer Award from IEEE Microwave Theory and Techniques Society in 2021.

REFERENCES

[1] U.S. Department of Commerce, Office of Spectrum Management, Frequency Allocation Chart, 2016. Accessed: Jul. 5, 2021. [Online]. Available: https://www.ntia.doc.gov/files/ntia/publications/january_2016_spectrum_wall_chart.pdf

[2] C. Sirtori, "Applied physics: Bridge for the terahertz gap," *Nature*, vol. 417, no. 6885, pp. 132–133, May 9, 2002. doi: 10.1038/417132b. PMID: 12000945.

[3] I. Mizuno and C.-C. Han, "JCMT opens new eyes on the universe," *Nature Astron.*, vol. 5, pp. 331–332, Mar. 2021.

[4] T. Nagatsuma *et al.*, "Sub-terahertz wireless communications technologies," in *Proc. 18th Int. Conf. Appl. Electromagn. Commun.*, 2005, pp. 1–4.

[5] W. Withayachumnankul, M. Fujita, and T. Nagatsu-ma, "Polarization responses of terahertz di-electric rod antenna arrays," in *Proc. Int. Conf. Microw. Millimeter Wave Technol.*, 2019, pp. 1–3.

[6] J. Bauer *et al.*, "A high-sensitivity AlGaN/GaN HEMT terahertz detector with integrated broad-band bow-tie antenna," *IEEE Trans. THz Sci. Technol.*, vol. 9, no. 4, pp. 430–444, Jul. 2019.

[7] A. Dyck *et al.*, "A transmitter system-in-package at 300 GHz with an off-chip antenna and GaAs-based MMICs," *IEEE Trans. THz Sci. Technol.*, vol. 9, no. 3, pp. 335–344, 2019.

[8] X. Wan, W. X. Jiang, H. F. Ma, and T. J. Cui "A broadband transformation optics metasurface lens," *Appl. Phys. Lett.*, vol. 104, no. 5, pp. 151601/1–151601/4, 2014.

[9] Y. Monnai *et al.*, "Terahertz beam steering and variable focusing using programmable diffraction gratings," *Opt. Exp.*, vol. 21, pp. 2347–2354, 2013.

[10] R. Mendis, A. Nag, F. Chen, and D. M. Mittleman, "A tunable universal terahertz filter using artificial dielectrics based on parallel-plate waveguides," *Appl. Phys. Lett.*, vol. 97, no. 13, pp. 131106/1–131106/3, 2010.

[11] T. Nagatsuma, G. Ducournau, and C. C Renaud, "Advances in terahertz communications accelerated by photonics," *Nature Photon.*, vol. 10, pp. 371–379, 2016.

[12] K. Sengupta, T. Nagatsuma, and D. M Mittleman, "Terahertz integrated electronic and hybrid electronic–photonic systems," *Nature Electron.*, vol. 1, pp. 622–635, 2018.

[13] R. Al Hadi *et al.*, "A 1 k-pixel video camera for 0.7–1.1 terahertz imaging applications in 65-nm CMOS," *IEEE J. Solid-State Circuits*, vol. 47, no. 12, pp. 2999–3012, Dec. 2012.

[14] K. Sengupta, "Integrated circuits for terahertz communication beyond 100 GHz: Are we there yet?," in *Proc. IEEE Int. Conf. Commun. Workshops*, 2019, pp. 1–6.

[15] R. Jain, P. Hillger, J. Grzyb, and U. R Pfeiffer, "A 0.42 THz 9.2 dBm 64-pixel source-array SoC with spatial modulation diversity for computational terahertz imaging," in *Proc. IEEE Int. Solid-State Circuits Conf.*, 2020, pp. 440–442.

[16] Y. Mehta, S. Razavian, K. Schwarm, R. M. Spearrin, and A. Babakhani, "Terahertz gas-phase spectroscopy of CO using a silicon-based picosecond impulse radiator," in *Proc. Conf. Lasers Electro-Opt.*, 2020, pp. 1–2.

[17] D. Parveg *et al.*, "A 180-GHz CMOS down-converter MMIC for atmospheric remote sensing applications," in *Proc. IEEE 17th Top. Meeting Silicon Monolithic Integr. Circuits RF Syst.*, 2017, pp. 64–67.

[18] M. T. Ruggiero and J. A. Zeitler, "Resolving the origins of crystalline anharmonicity using terahertz time-domain spectroscopy and ab initio simulations," *J. Phys. Chem. B*, vol. 120, pp. 11733–11739, 2016.

[19] M. Walther, B. Fischer, M. Schall, H. Helm, and P. Uhd Jepsen, "Far-infrared vibrational spectra of all-trans, 9-cis and 13-cis retinal measured by THz time-domain spectroscopy," *Chem. Phys. Lett.*, vol. 332, pp. 389–395, 2000.

[20] T. Makihara *et al.*, "Ultrastrong magnon–magnon coupling dominated by antiresonant interactions," *Nature Commun*, vol. 12, pp. 1–9, 2021.

[21] K. Delfanazari, R. A. Klemm, H. J. Joyce, D. A. Ritchie, and K. Kadowaki, "Integrated, portable, tunable, and coherent terahertz sources and sensitive detectors based on layered superconductors," *Proc. IEEE*, vol. 108, no. 5, pp. 721–734, May 2020.

[22] J. Stake *et al.*, "Integrated terahertz electronics for imaging and sensing," in *Proc. 19th Int. Conf. Microw. Radar Wireless Commun.*, 2012, pp. 122–123, doi: 10.1109/MIKON.2012.6233504.

[23] C. Hsieh, Y. Hsieh, J. Lin, H. Chen, C. Yang, and J. Y. Liu, "Signal generation techniques in CMOS for millimeter-wave and terahertz applications," in *Proc. IEEE Int. Symp. Circuits Syst.*, 2019, pp. 1–5, doi: 10.1109/ISCAS.2019.8702069.

[24] J. Ye, T. Fang, Z. Zhang, L. Liu, J. Liu, and N. Wu, "A 343.2-348.9 GHz CMOS terahertz source with on-chip antennas," in *Proc. IEEE Int. Conf. Integr. Circuits, Technol. Appl.*, 2019, pp. 13–14.

[25] S. Razavian, M. Hosseini, Y. Mehta, and A. Babakhani, "Terahertz channel characterization using a broadband frequency comb radiator in 130-Nm SiGe BiCMOS," *IEEE Trans. THz Sci. Technol.*, vol. 11, no. 3, pp. 269–276, May 2021.

[26] S. Razavian and A. Babakhani, "Multi-spectral THz micro-Doppler radar based on a silicon-based picosecond pulse radiator," in *Proc. IEEE/MTT-S Int. Microw. Symp.*, 2020, pp. 787–790.

[27] S. Razavian and A. Babakhani, "A THz pulse radiator based on PIN diode reverse recovery," in *Proc. IEEE BiCMOS Compound Semicond. Integr. Circuits Technol. Symp.*, 2019, pp. 1–4.

[28] R. Han and E. Afshari, "A 260 GHz broadband source with 1.1 mw continuous-wave radiated power and eirp of 15.7 dbm in 65 nm CMOS," in *IEEE Int. Solid-State Circuits Conf. Dig. Tech. Papers*, 2013, pp. 138–139.

[29] M. M. Assefzadeh and A. Babakhani, "Broadband oscillator-free THz pulse generation and radiation based on direct digital-to-impulse architecture," *IEEE J. Solid-State Circuits*, vol. 52, no. 11, pp. 2905–2919, Nov. 2017.

[30] M. M. Assefzadeh and A. Babakhani, "Laser-free THz pulse sources," in *Proc. 42nd Int. Conf. Infrared, Millimeter, THz Waves*, 2017, pp. 1–4, doi: 10.1109/IRMMW-THz.2017.8067089.

[31] A. Townley *et al.*, "A fully integrated, dual channel, flip chip packaged 113 GHz transceiver in 28nm CMOS supporting an 80 Gb/s wireless link," in *Proc. IEEE Custom Integr. Circuits Conf.*, 2020, pp. 1–4.

[32] K. Sengupta and A. Hajimiri, "A 0.28 THz power-generation and beam-steering array in CMOS based on distributed active radiators," *IEEE J. Solid-State Circuits*, vol. 47, no. 12, pp. 3013–3031, Dec. 2012.

[33] K. Sengupta and A. Hajimiri, "A 0.28THz 4×4 power-generation and beam-steering array," in *Proc. IEEE Int. Solid-State Circuits Conf.*, 2012, pp. 256–258.

[34] K. Sengupta, D. Seo, and A. Hajimiri, "A terahertz imaging receiver in 0.13μm SiGe BiCMOS technology," in *Proc. Int. Conf. Infrared, Millimeter, THz Waves*, 2011, pp. 1-2, doi: 10.1109/irmmw-THz.2011.6105192.

[35] K. Sengupta and A. Hajimiri, "Distributed active radiation for THz signal generation," in *Proc. IEEE Int. Solid-State Circuits Conf.*, 2011, pp. 288–289, doi: 10.1109/ISSCC.2011.5746322.

[36] A. Maestrini *et al.*, "Design and characterization of a room temperature all-solid-state electronic source tunable from 2.48 to 2.75 THz," *IEEE Trans. THz Sci. Technol.*, vol. 2, no. 2, pp. 177–185, Mar. 2012.

[37] S.H. Choi, M. Urteaga, and M. Kim, "600 GHz InP HBT frequency multiplier," *Electron. Lett.*, vol. 51, no. 23, pp. 1928–1930, 2015.

[38] J. Dou, S. Jiang, J. Xu, and W. Wang, "Design of D-band frequency doubler with compact power combiner," *Electron. Lett.*, vol. 53, no. 7, pp. 478–480, 2017.

[39] J. V. Siles *et al.*, "Next generation solid-state broadband frequency-multiplied terahertz sources," in *Proc. IEEE Antennas Propag. Soc. Int. Symp.*, 2012, pp. 1–2.

[40] J. V. Siles, K. B. Cooper, C. Lee, R. H. Lin, G. Chattopadhyay, and I. Mehdi, "A new generation of room-temperature frequency-multiplied sources with up to 10× higher output power in the 160-GHz–1.6-THz range," *IEEE Trans. THz Sci. Technol.*, vol. 8, no. 6, pp. 596–604, Nov. 2018.

[41] X. Lv, J. Ouyang, Z. Zhou, Y. Xu, and B. Zhang, "A high efficiency 0.2THz doubler," in *Proc. Int. Conf. Microw. Millimeter Wave Technol.*, 2019, pp. 1–3.

[42] Q. Feng *et al.*, "A wideband high-efficiency 465-555 GHz frequency tripler," *Proc. Int. Conf. Microw. Millimeter Wave Technol.*, 2020, pp. 1–3.

[43] R. Fujimoto and M. Fujishima, "Device-modeling and circuit-design techniques for CMOS transceivers in THz region," in *Proc. IEEE 54th Int. Midwest Symp. Circuits Syst.*, 2011, pp. 1–4.

[44] J. Kim, S. Kim, K. Song, and J. Rieh, "A 300-GHz SPST switch with a new coupled-line topology in 65-nm CMOS technology," *IEEE Trans. THz Sci. Technol.*, vol. 9, no. 2, pp. 215–218, Mar. 2019.

[45] J. Oberhammer, "THz MEMS—Micromachining enabling new solutions at millimeter and submillimeter-wave frequencies (invited paper)," in *Proc. IEEE Asia Pacific Microw. Conf.*, 2017, pp. 81–84.

[46] J. Oberhammer, "Micromachined THz systems - Enabling the large-scale exploitation of the THz frequency spectrum," in *Proc. Asia-Pacific Microw. Conf.*, 2018, pp. 25–27, doi: 10.23919/APMC.2018.8617359.

[47] V. Sanphuang, N. K. Nahar, and J. L. Volakis, "MEMS tunable THz filters for sensing," in *Proc. IEEE Antennas Propag. Soc. Int. Symp.*, 2013, pp. 1130–1131.

[48] J. Ning, Y. J. Cheng, and Y. Fan, "325-400 GHz 2-D beam steering antenna based on MEMS micromachining technology," in *Proc. IEEE MTT-S Int. Microw. Workshop Ser. Adv. Mater. Processes RF THz Appl.*, 2020, pp. 1–3.

[49] A. Kundu, M.R. Kanjilal, and M. Mukherjee, "III–V super-lattice SPST/SPMT pin switches for THz communication: Theoretical reliability and experimental feasibility studies," *Microsyst. Technol.*, vol. 27, pp. 539–554, 2021. doi: 10.1007/s00542-018-4053-5.

[50] J. Moon, H. Seo, K. Son, J. Crowell, D. Le, and D. Zehnder, "Phase-change materials for reconfigurable RF applications," in *Proc. 74th Annu. Device Res. Conf.*, 2016, pp. 1–1, doi: 10.1109/DRC.2016.7548404.

[51] J. Moon *et al.*, "Phase-change RF switches with robust switching cycle endurance," in *Proc. IEEE Radio Wireless Symp.*, 2018, pp. 231–233.

[52] M. Wang, F. Lin, and M. Rais-Zadeh, "Need a change? Try gete: A reconfigurable filter using germanium telluride phase change RF switches," *IEEE Microw. Mag.*, vol. 17, no. 12, pp. 70–79, Dec. 2016.

[53] A. Léon *et al.*, "RF power-handling performance for direct actuation of germanium telluride switches," *IEEE Trans. Microw. Theory Techn.*, vol. 68, no. 1, pp. 60–73, Jan. 2020, doi: 10.1109/TMTT.2019.2946145.

[54] R. Caverly, *Microwave and RF Semiconductor Control Device Modeling*. Norwood, MA, USA: Artech House, 2016.

[55] Accessed: Jul. 12, 2021. [Online]. Available: https://menlomicro.com/products/rf

[56] Accessed: Jul. 12, 2021. [Online]. Available: https://www.analog.com/en/products/switches-multiplexers/mems-switches.html

[57] D. Pozar, *Microwave Engineering*, 4th ed. New York, NY, USA: Wiley, 2011.

[58] M. Kantanen, J. Holmberg, M. Varonen, and A. Rantala, "Digitally controlled vector modulator SiGe MMIC for millimeter-wave phased array applications," in *Proc. 11th German Microw. Conf.*, 2018, pp. 51–54, doi: 10.23919/GEMIC.2018.8335026.

[59] P. V. Testa, C. Carta, and F. Ellinger, "A 140–210 GHz low-power vector-modulator phase shifter in 130nm SiGE BiCMOS technology," in *Proc. Asia-Pacific Microw. Conf.*, 2018, pp. 530–532, doi: 10.23919/APMC.2018.8617631.

[60] H. H. Beverage, C. W. Rice, and E. W. Kellogg, "The wave antenna a new type of highly directive antenna," *J. Trans. Amer. Inst. Elect. Engineers*, vol. XLII, pp. 215–266, Jan.–Dec. 1923, doi: 10.1109/T-AIEE.1923.5060870.

[61] H. Yagi and S. Uda, "Projector of the sharpest beam of electric waves," *Proc. Imperial Acad. Imperial Acad.*, vol. 2 no. 2: pp. 49–52, Feb. 1926. doi: 10.2183/pjab1912.2.49.

[62] Samuel Silver. *Microwave Antenna Theory and Design, Volume 12 of MIT Radiation Laboratory Series*. New York, New York, USA: McGraw-Hill, 1949.

[63] A. Arora, C. G. Tsinos, B. S. Mysore R. S. Chatzinotas, and B. Ottersten, "Efficient algorithms for constant-modulus analog beamforming," *IEEE Trans. Signal Process.*, early access, Jul. 8, 2021, doi: 10.1109/TSP.2021.3094653.

[64] N. Li *et al.*, "A four-element 7.5–9-GHz phased-array receiver with 1–8 simultaneously reconfigurable beams in 65-nm CMOS," *IEEE Trans. Microw. Theory Techn.*, vol. 69, no. 1, pp. 1114–1126, Jan. 2021.

[65] E. Ng, Y. Beltagy, G. Scarlato, A. Ben Ayed, P. Mitran, and S. Boumaiza, "Digital predistortion of millimeter-wave RF beamforming arrays using low number of steering angle-dependent coefficient sets," *IEEE Trans. Microw. Theory Techn.*, vol. 67, no. 11, pp. 4479–4492, Nov. 2019.

[66] B. Zheng, L. Jie, J. Bell, Y. He, and M. P. Flynn, "A two-beam eight-element direct digital beamforming RF modulator in 40-nm CMOS," *IEEE Trans. Microw. Theory Techn.*, vol. 67, no. 7, pp. 2569–2579, Jul. 2019.

[67] E. Arnieri *et al.*, "An integrated radar tile for digital beamforming X-/Ka-Band synthetic aperture radar instruments," *IEEE Trans. Microw. Theory Techn.*, vol. 67, no. 3, pp. 1197–1206, Mar. 2019.

[68] B. Yang, Z. Yu, J. Lan, R. Zhang, J. Zhou, and W. Hong, "Digital beamforming-based massive MIMO transceiver for 5G millimeter-wave communications," *IEEE Trans. Microw. Theory Techn.*, vol. 66, no. 7, pp. 3403–3418, Jul. 2018.

[69] R. Munson, "Conformal microstrip antennas and microstrip phased arrays," *IEEE Trans. Antennas Propag.*, vol. 22, no. 1, pp. 74–78, Jan. 1974.

[70] A. Gallegro, F. Esposito, and M. Pallas, "Dipole antenna on a high-dielectric substrate," in *Proc. 1st Eur. Microw. Conf.*, 1969, pp. 387–390, doi: 10.1109/EUMA.1969.331921.

[71] Y. Yoshimura, "A microstripline slot antenna (short papers)," *IEEE Trans. Microw. Theory Techn.*, vol. TMTT-20, no. 11, pp. 760–762, Nov. 1972.

[72] J. Howell, "Microstrip antennas," in *Proc. Antennas Propag. Soc. Int. Symp.*, 1972, pp. 177–180, doi: 10.1109/APS.1972.1146932.

[73] Accessed: Jul. 14–2021. IEEE Xplore Search results, 'microstrip antennas.' [online]. Available: http://ieeexplore.ieee.org

[74] L. Shen and H. Kong, *Applied Electromagnetism*, 3rd ed. Boston, MA, USA: PWS Publishing, 1987.

[75] Y. He, Y. Chen, L. Zhang, S. Wong, and Z. N. Chen, "An overview of terahertz antennas," *China Commun.*, vol. 17, no. 7, pp. 124–165, Jul. 2020, doi: 10.23919/J.CC.2020.07.011.

[76] A. A. Samat *et al.*, "Surface current distribution and performance analysis of different feeding techniques for microstrip patch antenna," in *Proc. 13th Int. UNIMAS Eng. Conf.*, 2020, pp. 1–5, doi: 10.1109/EnCon51501.2020.9299340.

[77] X. Wu, H. Lu, and K. Sengupta, "Programmable terahertz chip-scale sensing interface with direct digital reconfiguration at sub-wavelength scales," *Nature Commun.*, vol. 10, 2019, Art. no. 2722. doi: 10.1038/s41467-019-09868-6.

[78] S. Venkatesh *et al.*, "A high-speed programmable and scalable terahertz holographic metasurface based on tiled CMOS chips," *Nature Electron.*, vol. 3, pp. 785–793, 2020. doi: 10.1038/s41928-020-00497-2.

[79] X. Wu, H. Lu, X. Lu, and K. Sengupta, "A programmable active THz electromagnetic surface on-chip for multi-functional imaging," in *Proc. IEEE/MTT-S Int. Microw. Symp.*, 2018, pp. 1464–1467.
[80] X. Wu and K. Sengupta, "Multi-functional, active and information processing antenna surfaces in chip-scale THz systems," in *Proc. 18th Int. Symp. Antenna Technol. Appl. Electromagn.*, 2018, pp. 1–3, doi: 10.1109/ANTEM.2018.8573011.
[81] K. Sengupta and A. Hajimiri, "Designing optimal surface currents for efficient on-chip mm-wave radiators with active circuitry," *IEEE Trans. Microw. Theory Techn.*, vol. 64, no. 7, pp. 1976–1988, Jul. 2016.
[82] K. Sengupta and A. Hajimiri, "Mutual synchronization for power generation and beam-steering in CMOS with on-chip sense antennas near 200 GHz," *IEEE Trans. Microw. Theory Techn.*, vol. 63, no. 9, pp. 2867–2876, Sep. 2015.
[83] K. Sengupta and X. Wu, "THz silicon systems on chip: EM-circuits-systems codesign approach," in *Proc. 42nd Int. Conf. Infrared Millimeter THz Waves*, 2017, pp. 1–3, doi: 10.1109/IRMMW-THz.2017.8067115.
[84] K. Sengupta, H. Saeidi, X. Lu, S. Venkatesh, and X. Wu, "Terahertz chip-scale systems," in *Proc. Eur. Conf. Opt. Commun.*, 2020, pp. 1–3, doi: 10.1109/ECOC48923.2020.9333156.
[85] K. Sengupta, "Universal terahertz integrated systems: Bridging the 'THz' and 'application' gap in the next decade," in *Proc. IEEE MTT-S Int. Microw. RF Conf.*, 2019, pp. 1–3.

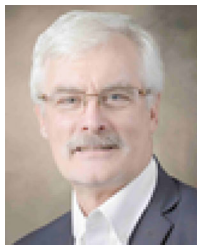

ROBERT H. CAVERLY (Life Fellow, IEEE) was born in Cincinnati, OH, USA, in 1954. He received the B.S.E.E and M.S.E.E degrees from the North Carolina State University, Raleigh, NC, USA, in 1978 and 1976, respectively, and the Ph.D. degree in electrical engineering from The Johns Hopkins University, Baltimore, MD, USA, in 1983. Since 1997, he has been a faculty member with the Department of Electrical and Computer Engineering, Villanova University, Villanova, PA, USA and is currently a Full Professor. Previously, he was with the University of Massachusetts Dartmouth (formerly Southeastern Massachusetts University), Dartmouth, MA, USA, for more than 14 years. He has authored or coauthored more than 100 journal and conference papers and two books *Microwave and RF Control Device Modeling* (2016) and *CMOS RFIC Design Principles* (2007), with Artech House, Norwood, MA, USA. His research interests include the characterization and modeling of semiconductor devices such as PIN diodes and FETs in the microwave and RF control environment. He is currently the Editor-in-Chief of *IEEE Microwave Magazine*, the Track Editor of IEEE JOURNAL OF MICROWAVES, and is a member of the Administrative Committee of the IEEE Microwave Theory and Techniques Society. From 2014 to 2016, he was a Distinguished Microwave Lecturer (DML) representing the MTT-S and is currently an Emeritus DML.